

Defective Majorana zero modes in non-Hermitian Kitaev chain

Xiao-Ming Zhao,¹ Cui-Xian Guo,^{1,2} Su-Peng Kou,² Lin Zhuang,³ and Wu-Ming Liu^{1,4,*}

¹*Beijing National Laboratory for Condensed Matter Physics,
Institute of Physics, Chinese Academy of Sciences, Beijing 100190, China*

²*Center for Advanced Quantum Studies, Department of Physics,
Beijing Normal University, Beijing 100875, China*

³*State Key Laboratory of Optoelectronic Materials and Technologies,
School of Physics, Sun Yat-Sen University, Guangzhou 510275, China*

⁴*Songshan Lake Materials Laboratory, Dongguan, Guangdong 523808, China*

Topological stability is an important property for topological materials. However, the non-Hermitian effects may change this situation. Here, we investigate the robustness of edge states in the non-Hermitian Kitaev chain with imbalanced tunneling term and superconducting pairing term. By defining the similarity of Majorana zero modes (MZMs) and magnetic factor, the coalescing phase diagram of the MZMs and corresponding spin polarization phase diagram are provided. Because of the non-Hermitian coalescence effect and non-Hermitian suppression effect induced by the breakdown of sublattice symmetry and particle-hole symmetry, the system emergence very interesting phenomenons, such as defective MZMs, number-anomalous bulk-boundary correspondence, coalescing of many-body ground states, the magnetic phase crossover without gap closing. Those novel non-Hermitian effects offer fresh insights into MZMs and topological physics.

I. INTRODUCTION

As a prototype model of one-dimensional (1D) topological superconductors (SCs), Kitaev chain have been a hot spot in condensed matter physics since unpaired Majorana zero modes (MZMs) are predicted to exist at the ends of this chain when the system is in the topologically nontrivial phase [1], which is robust for perturbation. Due to the potential applications in topological quantum computation (TQC), Majorana fermions or MZMs have been widely studied in recent years, including finding MZMs in different materials [2–9], its non-Abelian statistics [10–13] and its application in TQC [14–17].

Recently, non-Hermitian (NH) physics attracts lots of attention [18]. A non-Hermitian Hamiltonian has been introduced to describe the NH open system, which is regarded as a subsystem of an infinite Hermitian system [19]. The NH systems present many novel topological properties, such as exceptional points (EPs) in complex energy spectrum [20–22], anomalous topological transition [21–33] and edge states [34–37]. One of the most important properties for the topological systems is the bulk-boundary correspondence (BBC), i.e., bulk topological invariants of the bulk energy spectrum can predict unique gapless boundary states. Due to the NH skin effect [38–42], the typical BBC is broken, it obeys the non-Block BBC relationship [43–48]. Experimentally, those topological properties of the NH systems have been investigated in platform of photonics [49–53], quantum walks [54–56] and electric circuits [57].

While, it is still an open question whether the topological robustness of MZMs can be changed by the NH effects in superconducting systems. Physically, an NH

Kitaev chain can be obtained by setting the the chemical potential or hopping amplitude or SC paring to complex values, these choices may be realized by adding onsite particle gain/loss [58–64], or introducing nonreciprocal effects to the nearest neighbor hopping amplitude [38, 39], or imbalanced tunneling of particle paring [65–68], respectively. In previous research about the MZMs in NH Kitaev chain, the BBC is no different from the Hermitian cases both for the located (gain/loss) and dislocated(imbalanced SC paring) NH effects. Experimentally, the Hermitian Kitaev model can be realized in nanowire [69] and the related PT-symmetric many-body system have been presented in Ref.[70], the nonreciprocal effects can also be realized by using a cavity array with passive nearest neighbor tunneling [71]. Specifically, the NH Kitaev model with imbalanced particle paring may be realized by loading fermionic cold atoms in a 1D optical lattice, where the effective p-wave pairing can be induced by an optical Raman transition [72], and the non-Hermiticity may be implemented by controlling and monitoring the decay of atoms [73–76].

In this letter, we find that the breakdown of chiral symmetry and particle-hole (PH) symmetry can induce defective MZMs, which means one of the two localized edge states will disappear, referred to as number-anomalous of the MZMs. As a result, the conventional BBC is broken down, this indicates the NH effects break the robustness of the topological Majorana bound states. Here, the NH effects make difference are the coalescence effects and NH suppression effect. The coalescence effect means the similarity rate of two states $\gamma = \langle \psi_1 | \psi_2 \rangle$ changes from 0 to 1, i.e., two orthogonal states coalesce into one in a nonunitary way; For a target state $\psi = \alpha_1 |\uparrow\rangle + \alpha_2 |\downarrow\rangle$, the NH suppression effect means the NH parameters change the population of $|\uparrow\rangle$ and $|\downarrow\rangle$ in a non-unitary way.

This paper is organized as follows. In Sec.II, we describe the model Hamiltonian and analyze its topological

*Corresponding author; Electronic address: wliu@iphy.ac.cn

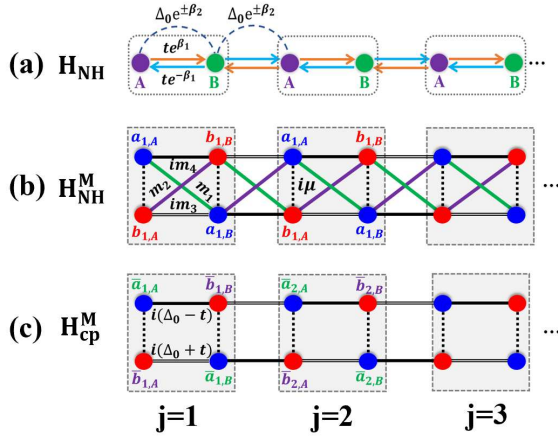


FIG. 1: Schematic illustration of the non-Hermitian Kitaev chain in different representation, the dotted box indicates the unit cell. (a) The lattice structure in Dirac Fermion representation, which is described by H_{NH} . The imbalanced hopping amplitudes from A to B (orange arrow) and from B to A (blue arrow) are described by β_1 ; The imbalanced pairing amplitudes of particles and holes are described by β_2 . (b) Kitaev chain viewed as two coupled SSH chains in Majorana representation, which is described by H_{NH}^{M} . The Majorana Fermion $a_{j,A/B}$ ($b_{j,A/B}$) are marked by blue (red) filled circle. The solid lines indicate the couplings m_1, m_2, im_3, im_4 between nearest neighbor sites, and the dashed lines indicate the couplings $i\mu$ intra-site. (c) The lattice schematic diagram of the Hermitian counterpart systems in Majorana representation, which is described by H_{cp}^{M} .

invariant. In Sec.III, we investigate the MZMs based on effective edge states Hamiltonian in the Majorana representation, and the number-anomalous BBC is revealed. In Sec.IV, we study the NH effects on the defective MZMs in spin language and show the phase crossover in the corresponding NH Ising model. Finally, we provide a summary and discussion in Sec.V.

II. NON-HERMITIAN KITAEV CHAIN AND TOPOLOGICAL INVARIANT

A. Hamiltonian of non-Hermitian Kitaev model

We introduce a 1D NH Kitaev model induced by the breakdown of chiral symmetry and particle-hole symmetry, the Hamiltonian is

$$H_{\text{NH}} = - \sum_j [t_L c_j^\dagger c_{j+1} + t_R c_{j+1}^\dagger c_j + \Delta^+ c_j^\dagger c_{j+1}^\dagger + \Delta^- c_{j+1} c_j + \mu(1 - 2n_j)], \quad (1)$$

where c_j^\dagger (c_j) is a fermionic creation (annihilation) operator on site j . As shown in Fig.1(a), we introduce the imbalanced hopping strength β_1 and the imbalanced SC

paring strength β_2 in the system, which has two sublattice in a unit cell. $t_{L/R} = te^{\pm\epsilon\beta_1}$ denote the left/right hopping amplitude where $\epsilon = \pm 1$ for inter/intra cell. $\Delta^\pm = \Delta_0 e^{\pm\beta_2}$ is the amplitude of p -wave pair creation (annihilation), μ is the chemical potential.

Then, we rewrite H_{NH} in the Bogoliubov-de Gennes formalism $H_{\text{NH}} = C^\dagger h_{\text{BdG}} C$ where C and C^\dagger are column and row vectors containing all canonical operators

$$C = (c_{1,A}, \dots, c_{N,B}, c_{1,A}^\dagger, \dots, c_{N,B}^\dagger)^T, \\ C^\dagger = (c_{1,A}^\dagger, \dots, c_{N,B}^\dagger, c_{1,A}, \dots, c_{N,B}). \quad (2)$$

then we can transform it to its Hermitian counterpart using a similarity transformation

$$h_{\text{cp}} = S_2 S_1 h_{\text{BdG}} S_1^{-1} S_2^{-1} \quad (3)$$

where the transform matrices are defined as

$$S_1 = \text{diag}\{1, r_1, \dots, 1, r_1, 1, r_1^{-1}, \dots, 1, r_1^{-1}\}, \\ S_2 = \text{diag}\{r_2, \dots, r_2, r_2^{-1}, \dots, r_2^{-1}\} \quad (4)$$

and $r_1 = \exp(-\beta_1)$, $r_2 = \exp[(\beta_1 - \beta_2)/2]$. So the Hamiltonian of the Hermitian counterpart read as [65, 66]

$$H_{\text{cp}} = - \sum_j \{(td_{j+1}^\dagger d_j + \Delta_0 d_j^\dagger d_{j+1}^\dagger + h.c.) + \mu(1 - 2n_j)\}, \quad (5)$$

where the canonical operators are defined as

$$d_j \equiv \Omega_j c_j, d_j^\dagger \equiv \Omega_j^{-1} c_j^\dagger \quad (6)$$

and the scale factors of similar transformation are

$$\Omega_{j \in \text{odd}} = e^{(\beta_1 - \beta_2)/2}, \Omega_{j \in \text{even}} = e^{-(\beta_1 + \beta_2)/2}. \quad (7)$$

It is obvious that the operators satisfy the anti-commutation relations $\{d_i, d_j^\dagger\} = \delta_{ij}$, $\{d_i, d_j\} = \{d_j^\dagger, d_i^\dagger\} = 0$ and H_{cp} has the form of the 1D Hermitian Kitaev model.

By the Fourier transform, We can write down the Bogoliubov-de Gennes Hamiltonian in the momentum space as

$$H_{\text{NH}}(k) = -\frac{1}{2} C^\dagger h(k) C \quad (8)$$

where C and C^\dagger are column and row vectors containing all canonical operators, $C = (c_{k,A}, c_{k,B}, c_{-k,A}^\dagger, c_{-k,B}^\dagger)^T$, $C^\dagger = (c_{k,A}^\dagger, c_{k,B}^\dagger, c_{-k,A}, c_{-k,B})$, and the non-Hermitian matrix is

$$h(k) = \begin{pmatrix} -2\mu & e^{-\beta_1} K_+ & 0 & e^{\beta_2} X_+ \\ e^{\beta_1} K_- & -2\mu & -e^{\beta_2} X_- & 0 \\ 0 & -e^{-\beta_2} X_+ & 2\mu & -e^{\beta_1} K_+ \\ e^{-\beta_2} X_- & 0 & -e^{-\beta_1} K_- & 2\mu \end{pmatrix} \quad (9)$$

where $K_\pm = t(1 + e^{\pm ik})$, $X_\pm = \Delta_0(1 - e^{\pm ik})$. Diagonalizing $h(k)$, we can get the energy dispersion

$$E(k) = \pm 2\sqrt{(t \cos(k) - \mu)^2 + \Delta^2 \sin^2(k)}, \quad (10)$$

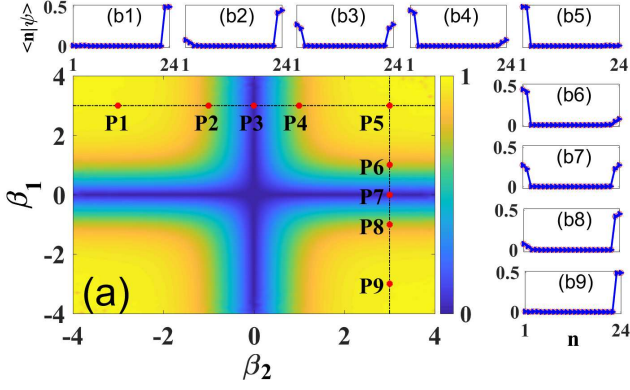


FIG. 2: Similarity γ_M and localized properties of the two defective MZMs with $L = 24$, $\mu = 0.1$, $t = 1$ and $\Delta_0 = 0.8$. (a) The blue area represent $\gamma_M = 0$ which means two MZMs local at two end of the chain independently, the yellow areas represent $\gamma_M = 1$ which means the two MZMs coalesce to one and local at either left or right end of the chain. (b1-b9) The distributions of the MZMs for different cases marked by the points P1-P9 in (a), respectively. For the cases in P1, P5, P9, which are away from $\beta_1 = 0$ and $\beta_2 = 0$, the two MZMs coalesce to one.

which can't be affected by the non-Hermitian parameter β_1, β_2 and is just the spectrum of $\beta_1 = \beta_2 = 0$. It should be noticed that there is no skin effect for the system [38–42]. Therefore, one can calculate the gap closing point $E(k) = 0$ to get the topological phase boundary of the system. As a result, the Majorana edge modes emerge in the topological phase $|\mu/t| < 1$.

B. Biorthogonal Z_2 topological invariant

Then, we investigate the topological properties of the NH Kitaev chain H_{NH} . The fermion Hamiltonian in momentum space is divided into three parts,

$$\hat{H}_{\text{NH}} = \hat{H}_{\text{NH},k>0} + \hat{H}_{\text{NH},k=0} + \hat{H}_{\text{NH},k=\pi}. \quad (11)$$

After diagonalizing the fermion Hamiltonian at the points $k > 0$, we have

$$\hat{H}_{\text{NH},k>0} = \sum_{k>0} \varepsilon(k) \alpha_k^\dagger \alpha_k - \sum_{k>0} \varepsilon(k) \alpha_{-k} \alpha_{-k}^\dagger \quad (12)$$

where α_k are diagonalized quasi-particles operators and $\alpha_{\pm k}$ annihilate the ground state $|G\rangle$, i.e., $\alpha_{\pm k}|G\rangle = 0$. Both α band has a positive energy at each point in momentum space $k > 0$. The Hamiltonian at $k = 0$ and $k = \pi$ are diagonalized into

$$\begin{aligned} \hat{H}_{\text{NH},k=0} &= \varepsilon(k=0) \alpha_{k=0}^\dagger \alpha_{k=0}, \\ \hat{H}_{\text{NH},k=\pi} &= \varepsilon(k=\pi) \alpha_{k=\pi}^\dagger \alpha_{k=\pi} \end{aligned} \quad (13)$$

where $\varepsilon(k=0) = \mu - t$ and $\varepsilon(k=\pi) = \mu + t$.

Based on the biorthogonal set, the right/left eigenstates and corresponding eigenvalues for the NH systems satisfy the relationship $\hat{H}_{\text{NH}}|\Psi_m^{\text{R}}\rangle = E_m|\Psi_m^{\text{R}}\rangle$, and $\hat{H}_{\text{NH}}^\dagger|\Psi_m^{\text{L}}\rangle = E_m^*|\Psi_m^{\text{L}}\rangle$. To describe this topological structure of \hat{H}_{NH} , we define *biorthogonal Z_2 topological invariant*,

$$\omega = \text{sgn}(\eta_{k=0} \cdot \eta_{k=\pi}) \quad (14)$$

where

$$\begin{aligned} \eta_{k=0} &= \langle \Psi_0^{\text{L}} | c_{k=0}^\dagger c_{k=0} | \Psi_0^{\text{R}} \rangle, \\ \eta_{k=\pi} &= \langle \Psi_0^{\text{L}} | c_{k=\pi}^\dagger c_{k=\pi} | \Psi_0^{\text{R}} \rangle. \end{aligned} \quad (15)$$

Here, $|\Psi_0^{\text{R}}\rangle$ denotes the ground state, $\Delta_0 = t$, and

$$\begin{aligned} \eta_{k=0} &= \frac{\varepsilon[k=0]}{|\varepsilon[k=0]|} = \frac{\mu - t}{|\mu - t|}, \\ \eta_{k=\pi} &= \frac{\varepsilon[k=\pi]}{|\varepsilon[k=\pi]|} = \frac{t + \mu}{|t + \mu|}. \end{aligned} \quad (16)$$

As a results, we have

$$\begin{aligned} \eta_{k=0} &= \begin{cases} +1, & \varepsilon(k=0) > 0 \\ -1, & \varepsilon(k=0) < 0 \end{cases}, \\ \eta_{k=\pi} &= \begin{cases} +1, & \varepsilon(k=\pi) > 0 \\ -1, & \varepsilon(k=\pi) < 0 \end{cases}. \end{aligned} \quad (17)$$

Then ω becomes topological invariant to characterize the universal properties of different topological phases, $\omega = 1$ with $(\eta_{k=0}, \eta_{k=\pi}) = (-1, -1)$ or $(1, 1)$ represent two trivial SCs, and $\omega = -1$ with $(\eta_{k=0}, \eta_{k=\pi}) = (-1, 1)$ or $(1, -1)$ represent two topological SCs, where there exist two MZMs located at two end of the 1D Kitaev chain.

III. DEFECTIVE MAJORANA EDGE STATES

A. Hamiltonian in Majorana representation

By introduce Majorana Fermion $a_n = c_n^\dagger + c_n$, $b_n = -i(c_n^\dagger - c_n)$, the non-Hermitian Hamiltonian H_{NH} can be written in Majorana-representation:

$$\begin{aligned} H_{\text{NH}}^{\text{M}} &= -\frac{1}{4} \sum_j [m_1(a_{j,A}a_{j,B} - b_{j,B}b_{j+1,A}) \\ &+ m_2(b_{j,A}b_{j,B} - a_{j,B}a_{j+1,A}) \\ &+ im_3(b_{j,A}a_{j,B} + b_{j,B}a_{j+1,A}) \\ &+ im_4(-a_{j,A}b_{j,B} - a_{j,B}b_{j+1,A}) \\ &+ i4\mu(a_{j,A}b_{j,A} + a_{j,B}b_{j,B})], \end{aligned} \quad (18)$$

where the coupling m_1, m_2, im_3, im_4 between nearest neighbor sites are:

$$\begin{aligned} m_1 &= t \sinh(\beta_1) + \Delta_0 \sinh(\beta_2), \\ m_2 &= t \sinh(\beta_1) - \Delta_0 \sinh(\beta_2), \\ m_3 &= t \cosh(\beta_1) + \Delta_0 \cosh(\beta_2), \\ m_4 &= -t \cosh(\beta_1) + \Delta_0 \cosh(\beta_2). \end{aligned} \quad (19)$$

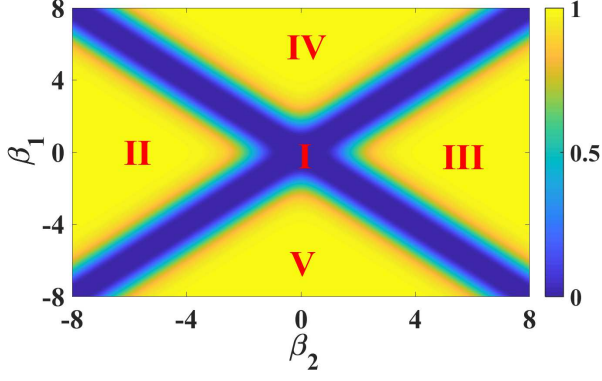


FIG. 3: Similarity γ_{spin} of the two ground states in spin-representation with $L = 4$, $t = \Delta_0 = 1$ and $\mu = 0.1$. The blue area I represents $\gamma_{\text{spin}} = 0$ which means the two ground states are orthogonal, The yellow area II-V represent $\gamma_{\text{spin}} = 1$ which means the two ground states coalesce to one and act as exceptional points (EPs).

As shown in Fig.1(b), the system contains four Majorana Fermions in each unit cell. the Majorana Fermion $a_{j,A/B}$ ($b_{j,A/B}$) are marked by blue (red) filled circle, the solid lines indicate the couplings m_1, m_2, im_3, im_4 between nearest neighbor sites, and the dashed lines indicate the couplings $i\mu$ intra-site.

B. Analytic results of the defective MZMs

To acquire the correspondence of topological number \mathcal{Z} and the number of edge states for the finite size chain $\mathcal{C}_{\text{finite}}$, we can investigate the analytic expression of edge states under the open boundary condition. We begin from the zero-mode eigenstates in the semi-infinite limit from the right or left boundary.

In order to avoid confusion with the operators c_j, c_j^\dagger in H_{NH} , we rewrite it's Hermitian counterpart H_{cp} in Eq.(5) by substituting the notation simply: $\{d_j, d_k^\dagger\} \rightarrow \{\bar{c}_j, \bar{c}_k^\dagger\}$, i.e., $H_{\text{cp}} = \bar{C}^\dagger h_{\text{cp}} \bar{C}$, which is written as

$$H_{\text{cp}} = - \sum_j \{ (t\bar{c}_{j+1}^\dagger \bar{c}_j + \Delta_0 \bar{c}_j^\dagger \bar{c}_{j+1}^\dagger + h.c.) - \mu(1 - 2\bar{n}_j) \}, \quad (20)$$

this is just the 1D Hermitian Kitaev model. Therefore, we can investigate the non-Hermitian properties of H_{NH} based on its Hermitian counterpart H_{cp} , with the definition of Majorana operators

$$\bar{c}_j^\dagger = \frac{1}{2}(\bar{a}_j + i\bar{b}_j), \bar{c}_j = \frac{1}{2}(\bar{a}_j - i\bar{b}_j) \quad (21)$$

we rewrite the Hamiltonian H_{cp} by Majorana operators,

$$H_{\text{cp}}^{\text{M}} = \frac{-i}{2} \sum_{j=1}^L \{ (t - \Delta_0) \bar{b}_{j+1} \bar{a}_j + (t + \Delta_0) \bar{b}_j \bar{a}_{j+1} + 2\mu \bar{a}_j \bar{b}_j \} \quad (22)$$

The lattice schematic diagram of H_{cp}^{M} is shown in Fig.1(c). As we know, in the Hermitian cases, two unpaired Majorana zero mode would locate at the right and left end of the Kitaev chain. Besides, for a finite size chain with $\mu \neq 0$, the eigne energy of the two Majorana edge modes can split due to the coupling of them.

Next, we try to acquire the analytic expression for the edge states. Firstly, we consider a very long wire, which means the Majorana edges modes have zero energy; We calculate their wave functions by using the Heisenberg equations of motion

$$[H_{\text{cp}}^{\text{M}}, \bar{a}_m] = 0, [H_{\text{cp}}^{\text{M}}, \bar{b}_m] = 0, \quad (23)$$

where \bar{a}_m, \bar{b}_m are the two Majorana operators at site n which were denoted by $\bar{a}_{n,A}, \bar{a}_{n,B}$ and $\bar{b}_{n,A}, \bar{b}_{n,B}$ above. We obtain the difference equations for these operators as [80, 81]:

$$\begin{aligned} (t + \Delta_0) \bar{b}_m + (t - \Delta_0) \bar{b}_{m+1} + 2\mu \bar{b}_m &= 0 \\ (t - \Delta_0) \bar{a}_m + (t + \Delta_0) \bar{a}_{m+1} + 2\mu \bar{a}_m &= 0 \end{aligned} \quad (24)$$

for $2 \leq m \leq 2L - 1$, These difference equations can be solved exactly by using Z -transform methods. We introducing a power series

$$A(z) = \sum_{m=0}^{\infty} z^{-m} \bar{a}_m \equiv Z[\bar{a}_m] \quad (25)$$

where z is a complex variable. The function $A(z) = Z[\bar{a}_m]$ is called the Z -transform of \bar{a}_m . Taking the Z -transform of the above difference equation and using properties such

$$Z[\bar{a}_{m-1}] = z^{-1} A(z), Z[\bar{a}_{m+1}] = z A(z) - z \bar{a}_0 \quad (26)$$

\bar{a}_0 is a constant determined by boundary conditions, one can obtain a closed form expression for the Z -transform $A(z)$, given by:

$$A(z) = \frac{\bar{a}_0 z^2}{z^2 + \frac{\mu}{t - \Delta_0} z + \frac{t + \Delta_0}{t - \Delta_0}} \quad (27)$$

This Z -transform has a unique inverse, which is the exact solution to the difference equation. Thus the obtained wave function is

$$\bar{a}_m = \bar{a}_0 C^m \left[\cos(\theta m) + \frac{1}{\tan \theta} \sin(\theta m) \right] \quad (28a)$$

$$\bar{b}_m = \bar{b}_0 C^{-m} \left[\cos(\theta m) + \frac{1}{\tan \theta} \sin(\theta m) \right] \quad (28b)$$

where

$$C = \sqrt{\frac{t - \Delta_0}{t + \Delta_0}}, \theta = \arctan \frac{\sqrt{t^2 - \Delta_0^2 - \mu^2}}{\mu} \quad (29)$$

The entire model is equivalent to two coupled SSH like chains containing both the hopping parameters $i(\Delta_0 -$

t) and $i(\Delta_0 + t)$, as shown in Fig.1(c). Here, we only concentrate on the zero energy eigen states, the excited states in complex and is not important here. If $t > \Delta_0 > 0, \mu \neq 0$, the system has two gap states, one can get the analytical wave function of the zero energy mode (gap states) in Majorana-representation. Here we express the zero mode of H_{cp}^{M} in \bar{a} -sublattice and \bar{b} -sublattice as (i.e. the states in the left and right edges)

$$\begin{aligned} |\psi\rangle_a^L &= \sum_{m=0}^{L-1} \Lambda(m) |m\rangle \otimes \begin{pmatrix} \bar{a} \\ 0 \end{pmatrix} \\ |\psi\rangle_b^R &= \sum_{m=0}^{L-1} \Lambda(m) |L-m\rangle \otimes \begin{pmatrix} 0 \\ \bar{b} \end{pmatrix} \end{aligned} \quad (30)$$

where we set $\bar{a}_{0,A} = \bar{b}_{N,B} = 1, \Lambda(m) = C^m \Theta(m)$

$$\Theta(m) = \left[\cos(\theta m) + \frac{1}{\tan \theta} \sin(\theta m) \right]. \quad (31)$$

When the region we considerate is $\mu^2 < 4(t^2 - \Delta_0^2)$ predict an oscillatory exponential decay of the coefficients: $e^{-n/2\zeta}$ for $|\psi\rangle_{\bar{a}}$, where the decay length ζ is defined by

$$\zeta = 1 / \left| \ln \left(\frac{t - \Delta_0}{t + \Delta_0} \right) \right| \quad (32)$$

So with the inverse similarity transformation based on Eq. (6), Eq. (20) and Eq. (21), we exchange the operator by the rule $(\bar{a}_j, \bar{b}_j) \rightarrow (\bar{c}_j^\dagger, \bar{c}_j) \rightarrow (d_j^\dagger, d_j) \rightarrow (c_j^\dagger, c_j)$, and we get the anti-zero-energy modes (edge states) for the initial non-Hermitian Hamiltonian H_{NH} in Nambu representation, as shown in Eq.(2). The right-vectors of the right/left localized edge states are expressed as

$$\begin{aligned} |\psi_{\text{NH}}^{\text{R}}\rangle &= \frac{i}{\sqrt{\mathcal{N}_b}} \sum_{m=1}^L \Lambda(L-m+1) [\Omega_m^{-1} |m\rangle - \Omega_m |L+m\rangle], \\ |\psi_{\text{NH}}^{\text{L}}\rangle &= \frac{1}{\sqrt{\mathcal{N}_a}} \sum_{m=1}^L \Lambda(m) [\Omega_m^{-1} |m\rangle + \Omega_m |L+m\rangle], \end{aligned} \quad (33)$$

where $L = 2N$ is the length of the Majorana ladder, $\Omega_{m \in \text{odd}} = e^{(\beta_1 - \beta_2)/2}, \Omega_{m \in \text{even}} = e^{-(\beta_1 + \beta_2)/2}$.

Similarly, we can get the left-vector $\langle \Phi |$ of the zero mode edge states defined by $\langle \Phi | H = \langle \Phi | E$, or $H^\dagger | \Phi \rangle = E^* | \Phi \rangle$. We can use the exchange $te^{-\beta_1} \leftrightarrow te^{\beta_1}, \Delta_0 e^{\beta_2} \leftrightarrow \Delta_0 e^{-\beta_2}, \Omega \leftrightarrow \Omega^{-1}$, for convenience, the left-vector for the right/left localized edges states can be expressed as

$$\begin{aligned} \langle \Phi_{\text{NH}}^{\text{R}} | &= \frac{i}{\sqrt{\mathcal{N}_b}} \sum_{m=1}^L \Lambda(L-m+1) [\Omega_m |m\rangle - \Omega_m^{-1} |L+m\rangle], \\ \langle \Phi_{\text{NH}}^{\text{L}} | &= \frac{1}{\sqrt{\mathcal{N}_a}} \sum_{m=1}^L \Lambda(m) [\Omega_m |m\rangle + \Omega_m^{-1} |L+m\rangle], \end{aligned} \quad (34)$$

where $\mathcal{N}_a = \mathcal{N}_b = \sum_{m=1}^L 2\Lambda(m)^2 \equiv \mathcal{N}$ is biorthogonal normalization coefficient.

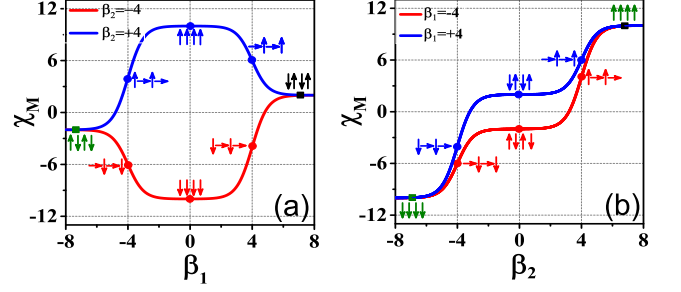


FIG. 4: The spin structure of the many-body ground state $|G\rangle_{\text{NH}}^1$ with (a) $\beta_2 = \pm 4$ and (b) $\beta_1 = \pm 4$. Here, we set $L = 4, t = \Delta_0 = 1$ and $\mu = 0.1$. The non-Hermitian suppression effect, induced by the competition of β_1 and β_2 , drives the spin flipping to opposite direction continuously without gap closing.

Next, taking $(|\psi_{\text{NH}}^{\text{R}}\rangle, |\psi_{\text{NH}}^{\text{L}}\rangle)$ and $(\langle \Phi_{\text{NH}}^{\text{L}} |, \langle \Phi_{\text{NH}}^{\text{R}} |)$ as the basis states, we construct the *effective Hamiltonian* of edge states for the finite-size Kitaev chain as

$$\mathcal{H}_{\text{edge}} = \begin{pmatrix} h_{\text{LL}} & h_{\text{LR}} \\ h_{\text{RL}} & h_{\text{RR}} \end{pmatrix}, \quad (35)$$

where the elements of $\mathcal{H}_{\text{edge}}$ are defined as $h_{\text{I,J}} = \langle \Phi_{\text{NH}}^{\text{I}} | H_{\text{NH}} | \psi_{\text{NH}}^{\text{J}} \rangle$ and I, J = L, R. We have $h_{\text{LL}} = h_{\text{RR}} = 0, h_{\text{RL}} = h_{\text{LR}}^* = i\xi$, i.e.,

$$\mathcal{H}_{\text{edge}} = \begin{pmatrix} 0 & -i\xi \\ i\xi & 0 \end{pmatrix} = \xi \sigma_y \quad (36)$$

where σ_y denotes the Pauli matrices acting on the subspace of two edge states and ξ is the coupling coefficient of them [82]:

$$\begin{aligned} \xi &= \frac{\sqrt{t^2 - \Delta_0^2}^{L+1}}{4 \sin^3 \theta} \{ 2 \sin(\theta L) \\ &\quad + L \sin[(L+2)\theta] - L \sin[(L+4)\theta] \} \end{aligned} \quad (37)$$

The energy of MZMs are $E_{\text{edge}}^\pm = \pm \sqrt{|\xi|}$ and in the thermodynamic limit ($L \mapsto +\infty$) we have $E_{\text{edge}}^\pm \mapsto 0$. Because the eigenstates of σ_y is $(1, i)$ and $(1, -i)$, the eigenstates of $\mathcal{H}_{\text{edge}}$ (i.e. the eigen wavefunction of edge states) are

$$\begin{aligned} |\psi^+\rangle &= \frac{1}{\sqrt{2\mathcal{N}}} (|\psi_{\text{NH}}^{\text{L}}\rangle + i |\psi_{\text{NH}}^{\text{R}}\rangle), \\ |\psi^-\rangle &= \frac{1}{\sqrt{2\mathcal{N}}} (|\psi_{\text{NH}}^{\text{L}}\rangle - i |\psi_{\text{NH}}^{\text{R}}\rangle). \end{aligned} \quad (38)$$

So far, we get the analytic solution of the non-Hermitian Majorana zero modes.

C. Number-anomalous bulk-boundary correspondence

Then, to describe the localization and the orthogonal-ity of the two edge states, i.e., to investigate the bulk-

boundary correspondence of the NH system, we define the similarity of the two edge states as

$$\gamma_M \equiv \langle \psi^- | \psi^+ \rangle = (e^{-\beta_1} - e^{\beta_1}) (e^{\beta_2} - e^{-\beta_2}) \kappa, \quad (39)$$

where $\kappa = \frac{1}{2^N} \sum_{n=0}^{L-1} (-1)^n C^{2n} \Theta_n^2$ is a nonzero value independent of β_1 and β_2 . When $\beta_{1,2} \neq 0$ we have $\gamma_M \neq 0$, which means the two edge states $|\psi^\pm\rangle$ are not orthogonal and no longer located at two ends of the chain respectively. The distributions of similarity $\gamma_M(\beta_1, \beta_2)$ and corresponding eigen wavefunction are calculated numerically and are shown in Fig.2. We can see that, γ_M tends to be 1 when the NH strength β_1 and β_2 are away from 0, this means the two MZMs become one gradually and evolve to the exceptional points (EPs) eventually. As a result, the typical BBC is broken and the MZM local only at the left or right end of the system. For example, when $\beta_1 = \beta_2 = 3$ (point P5 in Fig.2(a)), $\gamma_M = 1$ and the Majorana zero mode only locate at left end of the chain (shown in (b5) of Fig.2(b)).

Therefore, the number-anomalous BBC can be defined as [37]

$$\mathcal{C}_{\text{finite}} = 2 - \gamma_M. \quad (40)$$

In the Hermitian case ($\beta_1 = \beta_2 = 0$), we have $\gamma_M = 0$, the number of MZMs is $\mathcal{C}_{\text{finite}} = 2$ and the typical BBC is acquired. While, in the NH cases ($\beta_{1,2} \neq 0$), we have $0 < \gamma_M \leq 1$, the MZMs becomes defective and we have $1 \leq \mathcal{C}_{\text{finite}} \leq 2$. A special case is $\mathcal{C}_{\text{finite}} = 1$, which indicates the existence of a singular MZM. This phenomenon didn't occur in previous studies, neither in Hermitian nor in NH SC systems.

There are two reasons for this observation: the breakdown of sublattice symmetry induced by β_1 and the breakdown of the particle-hole symmetry induced by β_2 . As shown in the Fig.1(a), the imbalanced particle hopping lead to the breakdown of sublattice symmetry, which can suppress the particles located at A-sublattice ($\beta_1 < 0$) or B-sublattice ($\beta_1 > 0$). Meanwhile, the imbalanced pairing amplitudes lead to the breakdown of the particle-hole symmetry, which make the Majorana quasiparticle behave particle-like or hole-like. In a word, the defective Majorana zero modes are induced by the breakdown of sublattice symmetry and particle-hole symmetry.

IV. MANY-BODY CORRESPONDENCE OF THE DEFECTIVE MZMS

Benefit from the mapping between Kitaev chain and spin chain, one can simulate the MZMs in the Ising language via a Jordan-Wigner transformation [77, 78], because the Ising model is relatively easy to implement. For example, MZMs have attracted much attention due to their potential application in topological quantum computations, the spin chain can be used to simulate the braiding of these MZMs, which corresponding to the

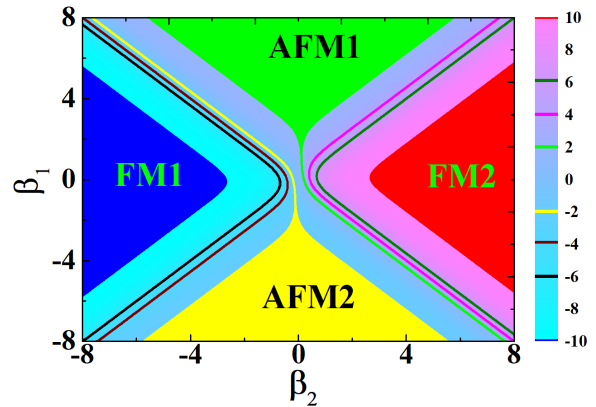


FIG. 5: Global magnetic phase diagram of the many-body ground states. The variations of χ_M induced by non-Hermitian suppression effect are marked by different colors: FM phase (blue and red area), AFM phase (green and yellow area) and so on. Here, we set $L = 4$, $t = \Delta_0 = 1$ and $\mu = 0.1$.

topological quantum gates [79]. Therefore, it is necessary to explore the many-body correspondence of the defective MZMs and explain the NH effects on the spin-representation.

A. NH spin model corresponding to the NH Kitaev model

In the Hermitian case, it has been noted that the Kitaev model can be mapped to the Ising model via the Jordan-Wigner transformation, and the two MZMs can also be mapped to the two degenerate ground states of the Ising model. Similarly, we can transform the NH Kitaev model to NH Ising model in this way. The Hamiltonian H_{NH} can be written in spin-representation as

$$H_{\text{NH}}^{\text{spin}} = -\frac{1}{4} \sum_j \{ J_1 \sigma_j^x \sigma_{j+1}^x + J_2 \sigma_j^y \sigma_{j+1}^y + i J_3 \sigma_j^x \sigma_{j+1}^y + i J_4 \sigma_j^y \sigma_{j+1}^x + 4\mu \sigma_j^z \}, \quad (41)$$

where

$$\begin{aligned} J_1 &= t \cosh \beta_1 + \Delta_0 \cosh \beta_2, \\ J_2 &= t \cosh \beta_1 - \Delta_0 \cosh \beta_2, \\ J_3 &= et \sinh \beta_1 + \Delta_0 \sinh \beta_2, \\ J_4 &= -et \sinh \beta_1 + \Delta_0 \sinh \beta_2. \end{aligned} \quad (42)$$

And $H_{\text{NH}}^{\text{spin}}$ can also be transformed to a Hermitian Hamiltonian by the similarity transformation

$$H_{\text{cp}}^{\text{spin}} = U H_{\text{NH}}^{\text{spin}} U^{-1}, \quad (43)$$

where the similarity transformation operator can be expressed as $U = \prod_j U_{j,A} \otimes U_{j,B}$, where

$$\begin{aligned} U_{j,A} &= \text{diag}\{1, \exp[(\beta_2 - \beta_1)/2]\}, \\ U_{j,B} &= \text{diag}\{1, \exp[(\beta_2 + \beta_1)/2]\}. \end{aligned} \quad (44)$$

	$ G\rangle_{\text{NH}}^1$	$ G\rangle_{\text{NH}}^2$	χ_{M}	γ_{spin}	Phase
$\beta_1 = 0, \beta_2 \rightarrow +\infty$	$ \uparrow\uparrow\uparrow\uparrow\rangle$	$ \uparrow\uparrow\uparrow\uparrow\rangle$	$L(L+1)/2$	1	FM2
$\beta_1 = 0, \beta_2 \rightarrow -\infty$	$ \downarrow\downarrow\downarrow\downarrow\rangle$	$ \downarrow\downarrow\downarrow\downarrow\rangle$	$-L(L+1)/2$	1	FM1
$\beta_2 = 0, \beta_1 \rightarrow +\infty$	$ \downarrow\uparrow\downarrow\uparrow\rangle$	$ \downarrow\uparrow\downarrow\uparrow\rangle$	$L/2$	1	AFM1
$\beta_2 = 0, \beta_1 \rightarrow -\infty$	$ \uparrow\downarrow\uparrow\downarrow\rangle$	$ \uparrow\downarrow\uparrow\downarrow\rangle$	$-L/2$	1	AFM2
$\beta_1 = \beta_2 > 0$	$ \rightarrow\uparrow\rightarrow\uparrow\rangle$	$ \leftarrow\uparrow\leftarrow\uparrow\rangle$	$L(L+2)/4$	0	Even-FM2
$\beta_1 = \beta_2 < 0$	$ \rightarrow\downarrow\rightarrow\downarrow\rangle$	$ \leftarrow\downarrow\leftarrow\downarrow\rangle$	$-L(L+2)/4$	0	Even-FM1
$\beta_1 = -\beta_2 < 0$	$ \uparrow\rightarrow\uparrow\rightarrow\rangle$	$ \uparrow\leftarrow\uparrow\leftarrow\rangle$	$L^2/4$	0	Odd-FM2
$\beta_1 = -\beta_2 > 0$	$ \downarrow\rightarrow\downarrow\rightarrow\rangle$	$ \downarrow\leftarrow\downarrow\leftarrow\rangle$	$-L^2/4$	0	Odd-FM1

TABLE I: The non-Hermitian effects on the two ground states in different limit cases (first collum). The spin configurations, magnetic factor χ_{M} , similarity rate γ_{spin} and magnetic phase are shown in collum 2-6, respectively.

Therefore, the Hermitian counterpart of H_{NH} in spin-representation can be expressed as

$$H_{\text{cp}}^{\text{spin}} = - \sum_{j=1}^{L-1} \{J_x \sigma_j^x \sigma_{j+1}^x + J_y \sigma_j^y \sigma_{j+1}^y - 2\mu \sigma_j^z\}, \quad (45)$$

where $J_{x/y} = t \pm \Delta_0$ and this is just the quantum XY spin chain and its extensions have been studied from many different perspectives.

B. Similarity of the two degenerate ground states

To characterize the properties of ground states, we calculate the magnetic factor when the system is in its ground state. Firstly, for simplicity and typicality, we consider the limit case $\mu = 0, t = \Delta_0$ where $H_{\text{cp}}^{\text{spin}}$ is exactly the Ising model without transverse field, the ground states of $H_{\text{cp}}^{\text{spin}}$ are described as

$$|G\rangle_{\text{cp}}^1 = |\rightarrow\rightarrow\rightarrow\cdots\rightarrow\rangle, |G\rangle_{\text{cp}}^2 = |\leftarrow\leftarrow\leftarrow\cdots\leftarrow\rangle. \quad (46)$$

So the ground states of initial NH spin chain can be obtained completely under the inverse similarity transformation:

$$|G\rangle_{\text{NH}}^1 = U^{-1} |G\rangle_{\text{cp}}^1, |G\rangle_{\text{NH}}^2 = U^{-1} |G\rangle_{\text{cp}}^2. \quad (47)$$

In fact, U_i act as a transverse field inner each site i . When we adjust β_1 and β_2 , the two ground states may construct different spin structure in the spin chain. Then, we define the similarity of the two ground states as

$$\gamma_{\text{spin}}(\beta_1, \beta_2) = \text{NH}^2 \langle G | G \rangle_{\text{NH}}^1, \quad (48)$$

After a tedious calculation, we can obtain

$$\gamma_{\text{spin}}(\beta_1, \beta_2) = \left(-\tanh\left[\frac{\beta_1 + \beta_2}{2}\right] \tanh\left[\frac{\beta_1 - \beta_2}{2}\right] \right)^{\frac{L}{2}} \quad (49)$$

Therefore, γ_{spin} will change with β_1 and β_2 . It is obvious that $|G\rangle_{\text{NH}}^1$ and $|G\rangle_{\text{NH}}^2$ are not always orthogonal. We study this phenomena in some limiting case: (1) when $\beta_1 = 0$, we have $\gamma_{\text{spin}}(0, \beta_2) = [\tanh(\frac{\beta_2}{2})]^L$; (2) When $\beta_2 = 0$, we have $\gamma_{\text{spin}}(\beta_1, 0) = [-\tanh(\frac{\beta_1}{2})]^L$; (3) when

$\beta_1 = \beta_2$, we have $\gamma_{\text{spin}}(\beta_1 = \beta_2) = 0$. Indeed, for spin systems with finite size, two ground states will coalesce when $\beta_1 \mapsto 0$ (or $\beta_2 \mapsto 0$). While, two ground states can't coalesce in the thermodynamic limit $L \mapsto \infty$, due to $\tanh(\beta_{1/2}) < 1$.

Now, we take 4-spin systems as an example and show the coalescence phase diagram in Fig.(3). We can see that $\gamma_{\text{spin}} \mapsto 0$ when the NH strengths are near $\beta_1 = \beta_2$ region, and $\gamma_{\text{spin}} \mapsto 1$ when β_1, β_2 are large enough which means the wave functions of the two degenerate ground states coalesce. This is very different from the similarity of MZM in Majorana representation shown in Fig.(2), where $\gamma_{\text{M}} \rightarrow 0$ in the region near $\beta_1 = 0$, or $\beta_2 = 0$.

C. Phase crossover without gap closing

An important question is why the coalescing phase diagram of MZMs shown in Fig.(2) is totally different from the coalescing phase diagram of spin ground states shown in Fig.(3), i.e.

$$\gamma_{\text{M}}(\beta_1, \beta_2) \neq \gamma_{\text{spin}}(\beta_1, \beta_2). \quad (50)$$

The key point is the correspondence of single-particle and the many-body systems. We know that the relation of MZMs and the ground states of spin system is

$$|G\rangle_{\text{NH}}^{1/2} = \hat{\psi}_{\text{NH}}^{\text{L/R}} |F\rangle, \quad (51)$$

where $|F\rangle$ is the many-body vacuum state in spin-representation, and it is also the many-body quantum state with occupied single particle states for $E < 0$ and empty single particle states for $E \geq 0$. Therefore, the single-body wave function $|\psi_{\text{NH}}^{\text{L/R}}\rangle$ shown in Eq.33 can't describe the many-body ground states absolutely, we must take $|F\rangle$ into account. Indeed, the NH terms perturb the vacuum background also, even they do not change the energy of the states.

To give a quantitative description for the spin configurations of the two ground states in the spin system, we define a magnetic factor as

$$\chi_{\text{M}}(\beta_1, \beta_2) \equiv \sum_{n=1}^L \text{NH}^1 \langle G | n \sigma_n^z | G \rangle_{\text{NH}}^1, \quad (52)$$

where a weighted sum of the spin of the n -th lattice is introduced. The introduction of the lattice number "n" can distinguish each site, so the magnetic factor $\chi_M(\beta_1, \beta_2)$ contains all spin information in each site. Then, we take the lattice size $L = 4$ as an example, and give the magnetic susceptibility and spin configurations of the many-body ground states $|G\rangle_{\text{NH}}^1$ for typical cases $\beta_2 = \pm 4$ in Fig.(4a) and $\beta_1 = \pm 4$ in Fig.(4b), where $L = 4, t = \Delta_0 = 1, \mu = 0.1$. Besides, we summarize the phase for different limit cases in Table I. We can see that the competition of β_1 and β_2 can drive the spin flipping to opposite direction continuously, this is the non-Hermitian suppression effect. Moreover the global magnetic order phase diagram of the many-body ground states are shown in Fig.5, which can be divided into five parts corresponding to the coalesce phase diagram: region II and III are ferromagnetic (FM1, FM2), region IV and V are antiferromagnetic (AF1, AF2), while region I are the transition area of those four phases.

It should be emphasized that the gap remains opened during the phase crossover. The non-Hermitian Hamiltonian $H_{\text{NH}}^{\text{spin}}$ can be transformed to a Hermitian Hamiltonian by the similarity transformation as shown in Eq.(43). Because the similarity transformation can not change the energy spectrum, the gap between the ground states and the first excited state don't vary with $\beta_{1/2}$, the phase diagram is obtained without gap closing.

V. CONCLUSION

We investigate the non-Hermitian effects on the Kitaev chain, whose hopping and superconductor pairing

strength are both imbalanced. The biorthogonal \mathcal{Z}_2 topological invariant and Majorana edge states are given analytically, these two imbalanced NH terms can induce defective Majorana edge states, which means one of the two localized edge states will disappear due to the NH suppression effect. As a result, the typical bulk-boundary correspondence is broken down. Besides, the defective edge states are mapped to the ground states of the non-Hermitian transverse field Ising model. With the definition of state-similarity and magnetic factor for the two ground states, the spin structure and the global phase diagrams are given, the FM-AFM crossover without gap closing is revealed. The novel non-Hermitian effects may provide a way to investigate MZMs and topological physics.

VI. ACKNOWLEDGMENTS

This work is supported by NSFC Grant No. 11674026, 11974053, 1217040237, 61835013, National Key R&D Program of China under grants No. 2016YFA0301500, Strategic Priority Research Program of the Chinese Academy of Sciences under grants Nos. XDB01020300, XDB21030300.

-
- [1] A. Y. Kitaev, Phys. Usp. **44**, 131 (2001).
 - [2] L. Fu, and C. L. Kane, Phys. Rev. Lett. **100**, 096407 (2008).
 - [3] V. Mourik, K. Zuo, S. M. Frolov, S. R. Plissard, E. P. A. M. Bakkers, and L. P. Kouwenhoven, Science **336**, 1003 (2012).
 - [4] M. T. Deng, C. L. Yu, G. Y. Huang, M. Larsson, P. Caroff, and H. Q. Xu, Nano. Lett. **12**, 6414 (2012).
 - [5] L. P. Rokhinson, X. Liu, and J. K. Furdyna, Nat. Phys. **8**, 795 (2012).
 - [6] J. Alicea, Rep. Prog. Phys. **75**, 076501 (2012)
 - [7] H. Mebrahtu, I. Borzenets, H. Zheng, Y. Bomze, A. I. Smirnov, S. Florens, H. U. Baranger, and G. Finkelstein, Nat. Phys. **9**, 732 (2013).
 - [8] S. Nadjperge, I. K. Drozdov, J. Li, H. Chen, S. Jeon, J. Seo, A. H. MacDonald, B. A. Bernevig, and A. Yazdani, Science **346**, 602 (2014).
 - [9] E. J. H. Lee, X. Jiang, M. Houzet, R. Aguado, C. M. Lieber, and S. D. Franceschi, Nat. Nano **9**, 79 (2014).
 - [10] N. Read, and D. Green, Phys. Rev. B **61**, 10267 (2000).
 - [11] D. A. Ivanov, Phys. Rev. Lett. **86**, 268 (2001).
 - [12] S. DasSarma, C. Nayak, and S. Tewari, Phys. Rev. B **73**, 220502(R) (2006).
 - [13] A. Stern, Nature (London) **464**, 187 (2010).
 - [14] B. Lian, X. Q. Sun, A. Vaezi, X. L. Qi, and S. C. Zhang, Proc. Natl. Acad. Sci. U.S.A. **115**, 10938 (2018).
 - [15] C. Nayak, S. H. Simon, A. Stern, M. Freedman, and S. DasSarma, Rev. Mod. Phys. **80**, 1083 (2008).
 - [16] Jay D. Sau, Roman M. Lutchyn, Sumanta Tewari, and S. Das Sarma, Phys. Rev. Lett. **104**, 040502 (2010).
 - [17] J. Alicea, Y. Oreg, G. Refael, F. von Oppen, and M. P. A. Fisher, Nat. Phys. **7**, 412 (2011).
 - [18] Y. Ashida, Z. Gong, and M. Ueda, Adv. Phys. **69**, 249 (2020).
 - [19] I. Rotter and J. P. Bird, Rep. Prog. Phys. **78**, 114001 (2015).
 - [20] E. J. Bergholtz, J.C. Budich, and F. K. Kunst, Rev. Mod. Phys. **93**, 015005 (2021)
 - [21] C. Yin, H. Jiang, L. Li, R. Lü, and S. Chen, Phys. Rev. A **97**, 052115 (2018).
 - [22] A. Ghatak and T. Das, J. Phys.: Condens. Matter **31**, 263001 (2019).
 - [23] M. S. Rudner and L. S. Levitov, Phys. Rev. Lett. **102**, 065703 (2009).
 - [24] K. Esaki, M. Sato, K. Hasebe, and M. Kohmoto, Phys. Rev. B **84**, 205128 (2011).

- [25] Y. C. Hu and T. L. Hughes, *Phys. Rev. B* **84**, 153101 (2011).
- [26] H. Shen, B. Zhen, and L. Fu, *Phys. Rev. Lett.* **120**, 146402 (2018).
- [27] S. Lieu, *Phys. Rev. B* **97**, 045106 (2018).
- [28] Z. Gong, Y. Ashida, K. Kawabata, K. Takasan, S. Higashikawa, and M. Ueda, *Phys. Rev. X* **8**, 031079 (2018).
- [29] C. H. Liu, H. Jiang, S. Chen, *Phys. Rev. B* **99**, 125103 (2019).
- [30] H. Jiang, C. Yang, and S. Chen, *Phys. Rev. A* **98**, 052116 (2018).
- [31] K. Kawabata, K. Shiozaki, M. Ueda, and M. Sato, *Phys. Rev. X* **9**, 041015 (2019).
- [32] H. Zhou and J. Y. Lee, *Phys. Rev. B* **99**, 235112 (2019).
- [33] F. K. Kunst and V. Dwivedi, *Phys. Rev. B* **99**, 245116 (2019).
- [34] D. Leykam, K. Y. Bliokh, C. Huang, Y. D. Chong, and F. Nori, *Phys. Rev. Lett.* **118**, 040401 (2017).
- [35] T. E. Lee, *Phys. Rev. Lett.* **116**, 133903 (2016).
- [36] K. Kawabata, K. Shiozaki, and M. Ueda, *Phys. Rev. B* **98**, 165148 (2018).
- [37] X. R. Wang, C. X. Guo, and S. P. Kou, *Phys. Rev. B* **101**, 121116(R) (2020)
- [38] S. Yao, and Z. Wang, *Phys. Rev. Lett.* **121**, 086803 (2018).
- [39] S. Yao, F. Song, and Z. Wang, *Phys. Rev. Lett.* **121**, 136802 (2018).
- [40] T. S. Deng and W. Yi, *Phys. Rev. B* **100**, 035102, (2019).
- [41] F. Song, S. Yao, and Z. Wang, *Phys. Rev. Lett.* **123**, 170401 (2019).
- [42] S. Longhi, *Phys. Rev. Research* **1**, 023013 (2019).
- [43] Y. Xiong, *J. Phys. Commun.* **2**, 035043 (2018).
- [44] F. K. Kunst, E. Edvardsson, J. C. Budich, and E. J. Bergholtz, *Phys. Rev. Lett.* **121**, 026808 (2018).
- [45] S. Lin, L. Jin, and Z. Song, *Phys. Rev. B* **99**, 165148 (2019); K. L. Zhang, H. C. Wu, L. Jin, and Z. Song, *Phys. Rev. B* **100**, 045141 (2019).
- [46] C. H. Lee and R. Thomale, *Phys. Rev. B* **99**, 201103(R) (2019).
- [47] L. Herviou, J. H. Bardarson, and N. Regnault, *Phys. Rev. A* **99**, 052118 (2019).
- [48] K. Yokomizo and S. Murakami, *Phys. Rev. Lett.* **123**, 066404 (2019).
- [49] J. M. Zeuner, M. C. Rechtsman, Y. Plotnik, Y. Lumer, S. Nolte, M. S. Rudner, M. Segev, and A. Szameit, *Phys. Rev. Lett.* **115**, 040402 (2015).
- [50] S. Weimann, M. Kremer, Y. Plotnik, Y. Lumer, S. Nolte, K. G. Makris, M. Segev, M. C. Rechtsman, and A. Szameit, *Nat. Mater.* **16**, 433 (2017).
- [51] M. A. Bandres, S. Wittek, G. Harari, M. Parto, J. Ren, M. Segev, D. N. Christodoulides, and M. Khajavikhan, *Science* **359**, 4005 (2018).
- [52] H. Zhou, C. Peng, Y. Yoon, C. W. Hsu, K. A. Nelson, L. Fu, J. D. Joannopoulos, M. Soljacic, and B. Zhen, *Science* **359**, 1009 (2018).
- [53] A. Cerjan, S. Huang, M. Wang, K. P. Chen, Y. Chong, and M. C. Rechtsman, *Nat. Photon.* **13**, 623 (2019).
- [54] L. Xiao, X. Zhan, Z. H. Bian, K. K. Wang, X. Zhang, X. P. Wang, J. Li, K. Mochizuki, D. Kim, N. Kawakami, W. Yi, H. Obuse, B. C. Sanders, and P. Xue, *Nat. Phys.* **13**, 1117 (2017).
- [55] K. Wang, X. Qiu, L. Xiao, X. Zhan, Z. Bian, B. C. Sanders, W. Yi, and P. Xue, *Nat. Commun.* **10**, 2293 (2019).
- [56] L. Xiao, T. Deng, K. Wang, G. Zhu, Z. Wang, W. Yi, P. Xue, *Nat. Phys.* **16**, 761 (2020).
- [57] T. Helbig, T. Hofmann, S. Imhof, M. Abdelghany, T. Kiessling, L. W. Molenkamp, C. H. Lee, A. Szameit, M. Greiter, and R. Thomale, *Nat. Phys.* **16**, 747 (2020).
- [58] X. Wang, T. Liu, Y. Xiong, and P. Tong, *Phys. Rev. A* **92**, 012116 (2015).
- [59] P. San-Jose, J. Cayao, E. Prada, and R. Aguado, *Sci. Rep.* **6**, 21427 (2016).
- [60] C. Yuce, *Phys. Rev. A* **93**, 062130 (2016).
- [61] Q. B. Zeng, B. Zhu, S. Chen, L. You, and Rong Lü, *Phys. Rev. A* **94**, 022119 (2016).
- [62] H. Menke, M. M. Hirschmann, *Phys. Rev. B* **95**, 174506 (2017).
- [63] K. Kawabata, Y. Ashida, H. Katsura, and M. Ueda, *Phys. Rev. B* **98**, 085116 (2018).
- [64] S. Lieu, *Phys. Rev. B* **100**, 085110 (2019).
- [65] C. Li, X. Z. Zhang, G. Zhang, and Z. Song, *Phys. Rev. B* **97**, 115436 (2018).
- [66] X. Z. Zhang and Z. Song, *Ann. Phys.* **339**, 109 (2013).
- [67] P. Matthews, P. Ribeiro, and A. M. García-García, *Phys. Rev. Lett.* **112**, 247001 (2014)
- [68] K. Yamamoto, M. Nakagawa, K. Adachi, K. Takasan, M. Ueda, and N. Kawakami, *Phys. Rev. Lett.* **123**, 123601 (2019)
- [69] M. Franz, *Nat. Nanotechnol.* **8**, 149 (2016).
- [70] Y. Ashida, S. Furukawa, and M. Ueda, *Nat. Commun.* **8**, 15791 (2017).
- [71] A. McDonald, T. Pereg-Barnea, and A. A. Clerk *Phys. Rev. X* **8**, 041031 (2018)
- [72] L. Jiang, T. Kitagawa, J. Alicea, A. R. Akhmerov, D. Pekker, G. Refael, J. I. Cirac, E. Demler, M. D. Lukin, and P. Zoller, *Phys. Rev. Lett.* **106**, 220402 (2011).
- [73] T. E. Lee and C. K. Chan, *Phys. Rev. X* **4**, 041001 (2014);
- [74] T. E. Lee, F. Reiter, and N. Moiseyev, *Phys. Rev. Lett.* **113**, 250401 (2014).
- [75] Y. Ashida, S. Furukawa, and M. Ueda, *Phys. Rev. A* **94**, 053615 (2016).
- [76] J. Li, A. K. Harter, J. Liu, L. de Melo, Y. N. Joglekar, and L. Luo, *Nat. Commun.* **10**, 855 (2019).
- [77] E. H. Lieb, T. Schulz, D. C. Mattis, *Ann. Phys.* **16**, 407 (1961)
- [78] D. C. Mattis. *Phys. Today* **39**, 62 (1986).
- [79] J. S. Xu, K. Sun, Y. J. Han, C. F. Li, J. K. Pachos, and G. C. Guo, *Nat. Commun.* **7**, 13194 (2016)
- [80] S. Hegde, V. Shivamoggi, S. Vishveshwara, and D. Sen, *New Journal of Physics* **17**, 053036 (2015)
- [81] S. S. Hegde, S. Vishveshwara, *Phys. Rev. B*, **94**, 115166 (2016).
- [82] N. Leumer, M. Marganska, B. Muralidharan, and M. Grifoni, *J. Phys.: Condens. Matter* **32**, 445502 (2020).